Available online at www.sciencedirect.com
SCIENCE DIRECT®
Pergamon
Cement and Concrete Research 34 (2004) 789–797
CEMENT AND CONCRETE RESEARCH

Experimental study of micro/macro crack development and stress–strain relations of cement-based composite materials at elevated temperatures

Yu-Fang Fu[a], Yuk-Lung Wong[a,*], Chi-Sun Poon[a], Chun-An Tang[b], Peng Lin[c]

[a]*Department of Civil and Structural Engineering, The Hong Kong Polytechnic University, Hung Hom, Kowloon, Hong Kong, China*
[b]*CRISR, Northeastern University, Shenyang, Liaoning Province, 110006, China*
[c]*Department of Hydraulic and Hydroelectric Engineering, Tsing Hua University, Beijing 100083, China*

Received 17 March 2003; accepted 26 August 2003

Abstract

This paper presents the results of observations of scanning electron microscope (SEM) micro/macro crack development and simultaneous measurements of temperature-dependent stress–strain relations of hardened cement pastes (HCP) and mortar under a steady thermal state (up to 500 °C) and a displacement-controlled loading process. The experimental results showed that the thermal damage of HCP was not only due to the recognized decomposition of the hydration products but also to the formation of dehydration-induced microcracks. These damage mechanisms, together with three other types of macrocracks arisen from the mismatch of expansion/shrinkage between the phase materials (HCP and aggregates) contributed to the thermal damage of the mortar. By comparing the evolution of the stress–strain curves for the HCP and the companion mortar specimens, the effects of the damage mechanisms could be separately quantified. In this study, the thermal damage of the mortar specimens was largely caused by the thermal mismatch mechanism.

Keywords: Temperature; Crack; Stress–strain relation; Decomposition; SEM

1. Introduction

It has been recognized that the damage mechanisms of concrete at elevated temperatures are (i) thermal mismatch, (ii) pore pressure effects, and (iii) decomposition of hydrates [1]. The first two mechanisms induce stresses in the paste and the aggregates, and the last mechanism weakens the strength of the hydrates. Although active research work in these areas has been conducted for decades, it is still very difficult to quantitatively assess the thermal damages of concrete that is contributed by each of the mentioned three mechanisms, especially the thermal cracks of concrete induced during a heating process.

The temperature-dependent mechanical properties of normal strength concrete under a fire have been established in some design codes, such as CEB/FIP Model Code 90 [2]. In 1998, a state-of-the-art review on the mechanical properties of high-strength concrete at elevated temperatures was published [3]. However, the individual effects of the three identified damage mechanisms, which unavoidably coexist in the concrete test samples, are difficult to be distinguished. Attempts had been made to use the mechanical tests together with microstructural examinations of a heated hardened cement paste (a homogenous material) to quantify the relation between the decomposition of the hydrates and the strength deterioration of the paste material. In this respect, a number of semiempirical equations were developed which relate the compressive or tensile strengths of the paste with its porosity, details of which can be found in the literature [1]. It was suggested that the increase in porosity and coarsening of the pore size distribution (determined by means of MIP [mercury intrusion porosimetry]) were expected to cause strength reduction, particularly above 300 °C. Unfortunately, these experimental studies did not include similar tests on the companion mortar or concrete (a nonhomogenous two-phase material) samples. Otherwise, the effects of thermal mismatch and pore pressure on the strength degradation would have been identified.

Microstructural examinations using scanning electron microscope (SEM) provide useful visual observations on

* Corresponding author. Tel.: +852-27666009; fax: +852-23346389.
E-mail address: ceylwong@inet.polyu.edu.hk (Y.-L. Wong).

0008-8846/$ – see front matter © 2004 Elsevier Ltd. All rights reserved.
doi:10.1016/j.cemconres.2003.08.029

Table 1
Mix proportions of HCP and mortar specimens

Materials		HCP	Mortar
Water/cement ratio		0.5	0.5
Cement	Type	Ordinary Portland cement to BS 12: 1991	
	Density (kg/m^3)	3140	
	Content (kg)	500	500
Water (kg)		250	250
Fine aggregate sand (kg)		–	750
Size of specimen (mm)		20 × 10 × 3	20 × 10 × 3

the thermal decomposition of constitutive materials and the crack formation of concrete. Piasta [4] reported that the development of microcracks in a cement paste increased significantly beyond 300 °C. The cracks occurred firstly around calcium hydroxide $Ca(OH)_2$ crystals (at about 300 °C), and then around unhydrated large cement grains (at about 400 °C). Dias [5] indicated that the larger unhydrated cement grains tended to detach further from their shells of the hydrated products upon heating than those of the smaller cement grains. Lin et al. [6] further confirmed that only tiny cracks were developed along the boundary of calcium hydroxide crystals and unhydrated cement particles below 300 °C. The majority of the cracks and the large cracks were formed between 300 and 500 °C. Handoo et al. [7] also reported the deformation of the well-developed calcium hydroxide crystal $Ca(OH)_2$ and C-S-H gel in cooled concrete after it was exposed to high temperatures up to 600 °C. However, all these observations were carried out when the heated specimens were cooled to ambient temperatures. The crack/damage patterns so observed might be different from those right under high temperatures.

2. Research methodology and significance

In view of the abovementioned limitations, this paper describes the experimental study of compressive stress–strain relation of HCP and the companion mortar samples under a real-time SEM observation of the thermal cracking process of the test samples during heating up to 500 °C. The test samples were deliberately dried in an oven at 60 °C for 48 h before testing to minimize the effects of pore pressure on the thermal damages. Previous research [8] showed that the maximum radial temperature difference was directly proportional to the radius square of the specimen and the heating rate. The test samples in this study were then designed to be very small and thin (20 × 10 × 3 mm thick) so that a thermal steady state could be attained in a very short time, and the "structural effect" [9] or thermal gradient would be eliminated. Consequently, the damages of the HCP samples would

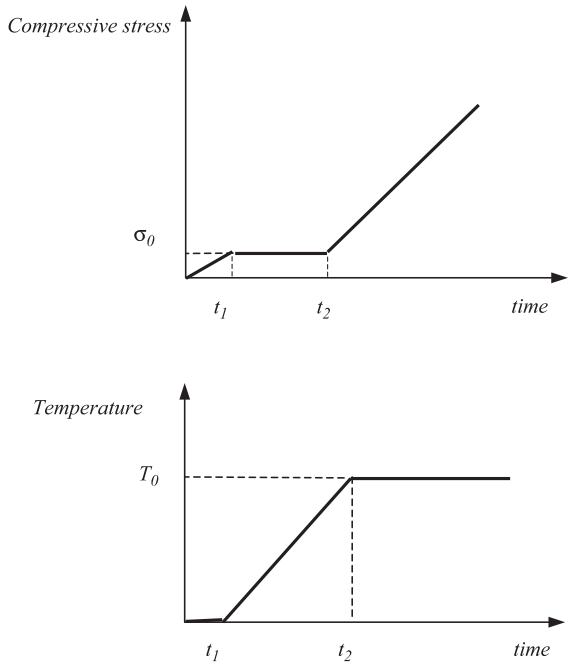

Fig. 2. Heating and loading regimes.

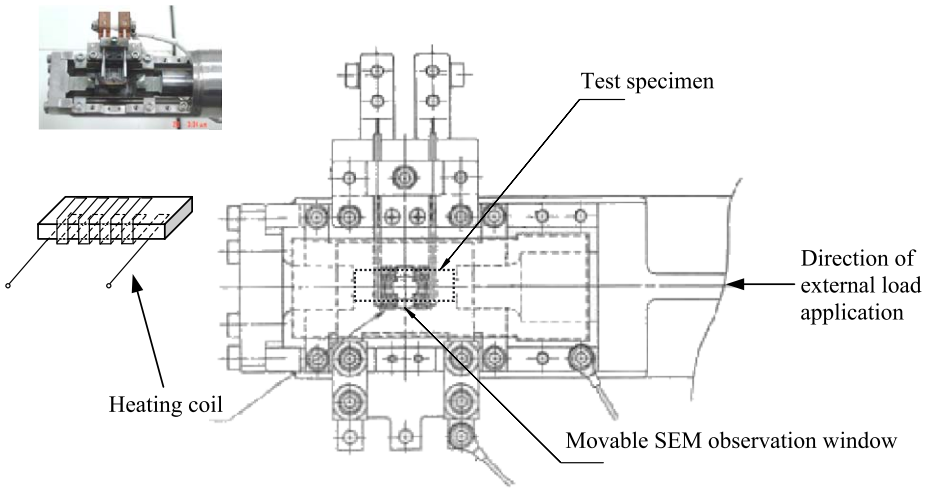

Fig. 1. Schematic of test setup.

be solely due to the thermal decomposition of the hydrates. The damages of the mortar samples were expected to be the result of both the thermal decomposition of the hydrates and the mismatch of the coefficients of thermal expansion (CTE) between the paste and the fine aggregates. By comparing the evolution of the stress–strain curves of the HCP and the mortar samples, quantitative assessments of the thermal decomposition and the mismatch in the thermal damage of the mortar samples was possible. Furthermore, as the load (thermal and external applied compression)–deformation behavior (in a macroscale), and the chemical decomposition and crack formation (in a microscale) of the HCP/mortar specimens during heating were observed in a real-time mode, a reliable visual picture and quantitative measurements of the thermal damage of the cementitious composite materials at high temperatures would be available to fill the knowledge gap in this area of study.

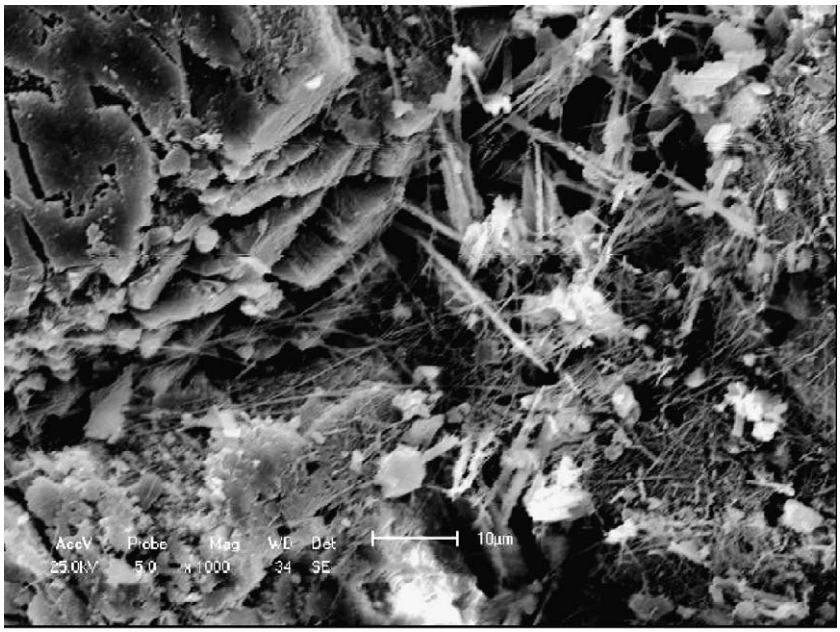

(a) Hardened cement paste, ×1000

(b) Mortar, ×600

Fig. 3. Morphology of typical HCP and mortar at room temperature.

3. Experiment details

3.1. Material and specimen preparation

One series of the hardened cement paste (HCP) and one series of the companion mortar specimens were prepared for testing. The mix proportions of the two test series and the dimensions of the specimens (20 × 10 × 3 mm) are shown in Table 1. To ensure the properties of the HCP, specimens were identical to those of the paste in the mortar specimens, the cement paste was prepared first. Then a portion of the paste mix was used to cast the HCP specimens. A fine uniformly graded river sand at the saturated surface dry condition were mixed with the remaining portion of the paste mix to form the mortar specimens. After 28-days water-curing at the temperature of 21 ± 2 °C, the specimens were polished and placed in an oven at a temperature of 60 °C for 96 h to attain a dry condition. The dried specimens were then coated with gold prior to the heating and loading tests in a SEM. To ensure consistency of the test results, at least two repetitive samples were examined for each case of study. The test series was denoted by 'C' or 'M' series for the HCP and the mortar specimens, respectively.

3.2. Equipment for testing and testing procedure

All specimens were tested using the high temperature fatigue-testing machine (HTFTM) of the Shimadzu Servopulser series. The equipment has three components: a servo-controlled load testing machine, a temperature controlled heating device, and a SEM of Super scan SS-550, that is capable of applying thermal and external loads on a specimen simultaneously. At the same time, the SEM can dynamically trace the change in microstructure and crack initiation/prop-

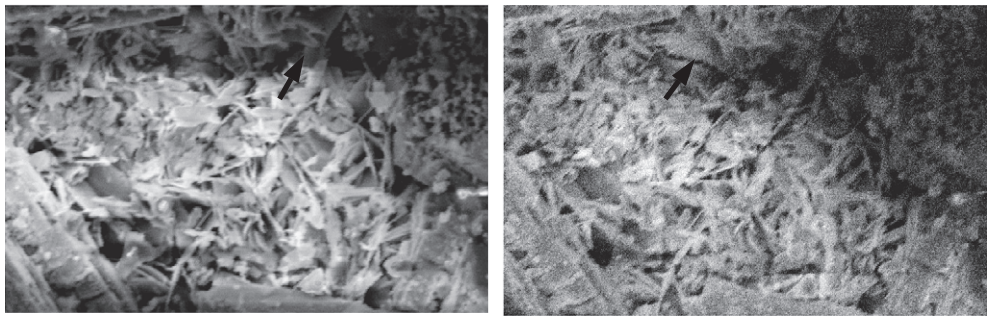

(a) Room temperature, ×450 (b) T=92°C, ×450

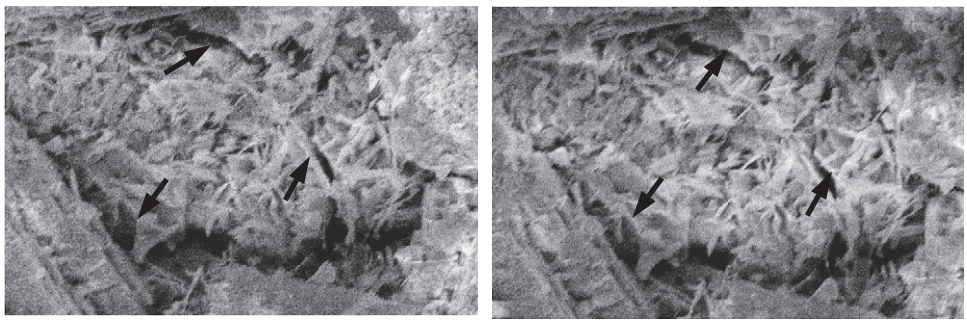

(c) T=148°C, ×450 (d) T=210°C, ×450

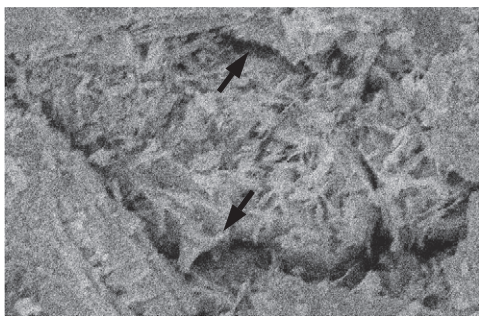

(e) T=310°C, ×450

Fig. 4. Changes in microstructure of hydration products in HCP (C-500) at elevated temperatures.

agation caused by the thermal and external compressive loads in a real-time mode. Fig. 1 shows the schematic of the test setup.

In this study, a steady thermal state test method was adopted to determine the mechanical properties of HCP and mortar specimens at elevated temperatures. Firstly, a test specimen was mounted in the heating chamber of the HTFTM with a constant clamping load of 0.2 kN, and was then heated to a target temperature ranging from 100 to 500 °C at a temperature increment of 100 °C at a rate of 4 °C per minute. During the heating up process, the 0.2 kN load would induce a constant compressive stress σ_0 of 6.67 MPa in the specimen. Once the target temperature was attained, a further uniaxial compressive load was applied to the speci-

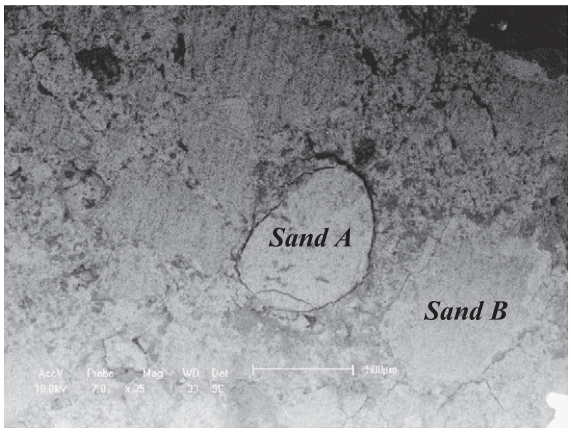

(a) Crack patterns at 300°C, ×35 in mortar (M-300)

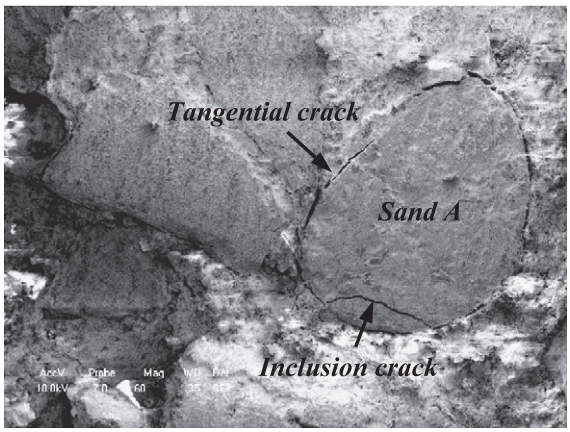

(b) Tangential and inclusion cracks at 300°C, ×60 in mortar (M-300)

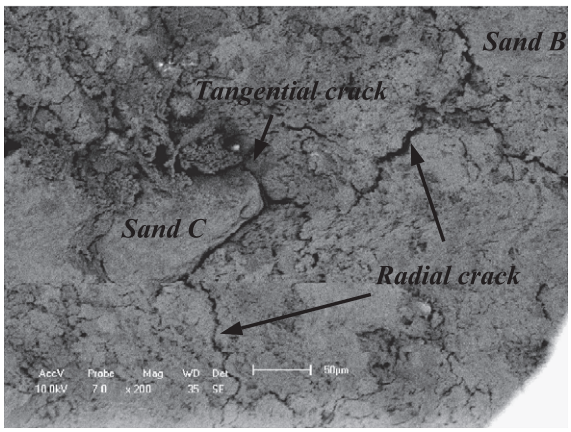

(c) Radial and tangential cracks at 300°C, ×120 in mortar (M-300)

Fig. 5. Thermal cracks in mortar specimen (M-300) at 300 °C.

men at the displacement rate of 0.001 mm/s till failure. During the entire period of heating and loading, the SEM was used to observe the thermal damage and the cracking process in a real-time mode. The SEM analyses were conducted using the Super scan SS-550 with an acceleration voltage between 10 and 25 kV. Due to the effects of high temperatures on electron movement, the micrograph quality decreases with increasing temperatures. A schematic heating process and loading process are shown in Fig. 2.

4. Experimental results

4.1. Morphology of HCP and mortar at room temperature

Fig. 3 shows two representative micrographs of the microstructures of the HCP and the mortar specimens at the age of 28 days before heating. Their compressive strengths were 76 and 66 MPa, respectively. The HCP specimen had a good framework of platelike calcium hydroxide crystals, needle- or fiberlike C-S-H and crystals of ettringite and pores. In the mortar specimen, no transition zone was observed between the cement paste and the sand.

4.2. Damage and crack patterns at elevated temperatures

4.2.1. HCP specimens

Fig. 4 shows the development of a damage/crack pattern, in a mesoscale, in the HCP specimen C-500 under increasing temperatures and a constant clamping load of 0.2 kN. In Fig. 4a, the calcium silicate hydrates, looked like small thin sheets, were well packed together at room temperature. At 92 °C, a fine crack (indicated by an arrow) occurred near the lower region of Fig. 4b. After reaching 148 °C, a tiny crack and a relative long crack were formed near the previous crack (Fig. 4c). As the temperature was further increased to 310 °C, the three identified cracks grew in length/width (Fig. 4d and e). Moreover, the microtexture of the matrix appeared to be coarsened with increasing temperatures, indicating changes in porosity. Since the hydrated cement was composed of various kinds of hydration products (C-S-H gel, Calcium hydroxide, C_2AH_8, C_3AH_6 and ettringite) that had different rates of dehydration/decomposition, and possibly different levels of thermal expansion/shrinkage with increasing temperatures, the cracks so observed were likely the results of thermal mismatch of the hydration products. We call these microcracks as dehydration-induced cracks. Piasta [4], Dias [5] and Lin et al. [6] also observed similar microcracks formed in their HCP specimens from the postheated SEM observations. However, the present study was the first real-time observation of the thermal microcracking process of HCP.

4.2.2. Mortar specimens

Fig. 5 depicts three typical mismatch-induced cracks (radial cracks, tangential cracks and inclusion cracks) around the sand aggregates in the mortar specimen M-300 at 300 °C under a constant clamping load of 0.2 kN (a compressive stress of 6.67 MPa). In experiments it was very difficult to keep the observation on the same location of the used specimen, because the specimen was expanding continuously. It also took time to take and save the picture on a computer. Although the micrographs obtained below 300 °C were not taken at the same location, all these cracks were definitely penetrated during the heating process, not preexisting flaws. This is because all these cracks were clear and nothing filled inside them.

It has been shown [10,11] that the radial cracks in the paste would occur when the CTE of the paste was smaller than that of the aggregate. On the other hand, the inclusion cracks in the aggregate and the tangential cracks at the paste–aggregate interface would form when the CTE of the paste was greater than that of the aggregate. Li et al. [12] and Simonin et al. [13] also reported that the microcracks at the interface between the HCP and the aggregates in the postheated concrete. The coexistence of three types of cracks in the test specimen at 300 °C can be explained with the help of Fig. 6.

Fig. 6 shows the typical thermal expansions of the HCP and mortar specimens. As expected, the thermal strain of the HCP initially increased with temperature. However, its strain started decreasing at above 100 °C, and eventually shrank with increasing temperatures. At 500 °C, the shrinkage of the HCP reached −2.3%. On the other hand, the thermal expansion of the mortar almost linearly increased with temperatures because of the continuous expansion of the sand aggregates. Its expansion at 500 °C attained 0.9%. Verbeck and Hass [14] reported that sand generally had a lower linear coefficient of thermal expansion at lower temperature, say below 100 °C, in comparison with HCP.

Consequently, as observed in Fig. 5, tangential cracks and inclusion cracks in the mortar specimen should be formed at a temperature less than 100 °C, and radial cracks should be formed at a higher temperature, from 200 to 300 °C. These cracks were evolved from the thermal mismatch between the sand aggregate and the HCP. Certainly, the effects of thermal decomposition of the hydration products and fine dehydra-

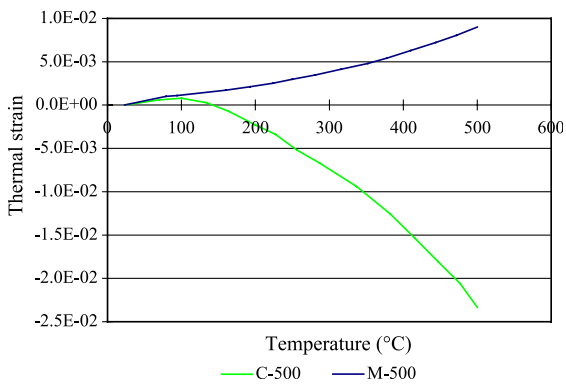

Fig. 6. Thermal expansions of HCP (C-500) and mortar (M-500).

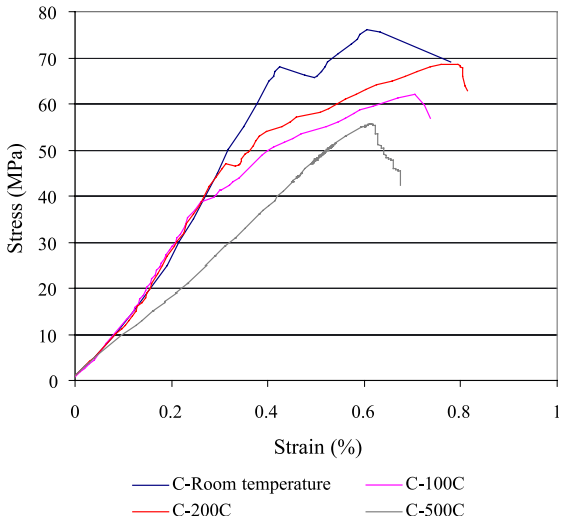

Fig. 7. Compressive stress–strain curves of HCP specimens at different temperature levels.

tion-induced cracks also existed in the HCP matrix of the mortar specimens. Therefore, thermal induced-damage of the mortar specimens is expected to be more severe than that of the paste specimens at a given elevated temperature, and this is confirmed by the following stress–strength studies.

4.3. Stress–strain relations

The compressive stress–strain relations of the HCP and mortar specimens determined under a thermal steady and displacement-rate conditions are shown in Figs. 7 and 8 respectively. From these measurements, the peak strengths and the secant modulus calculated at one third of the peak strength of the specimens are plotted in Fig. 9. The peak strengths and secant modulus decreased with increasing

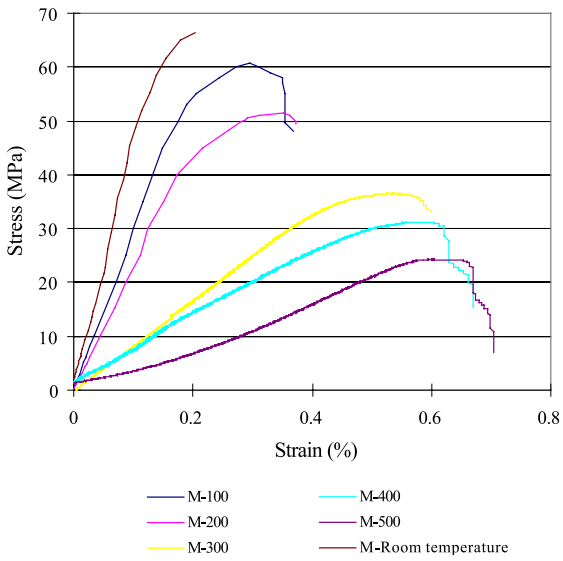

Fig. 8. Compressive stress–strain curves of mortar specimens at different temperature levels.

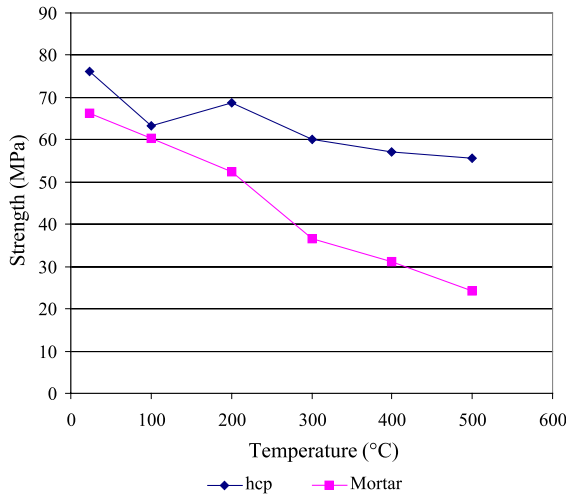

(a) Peak strength vs. temperature

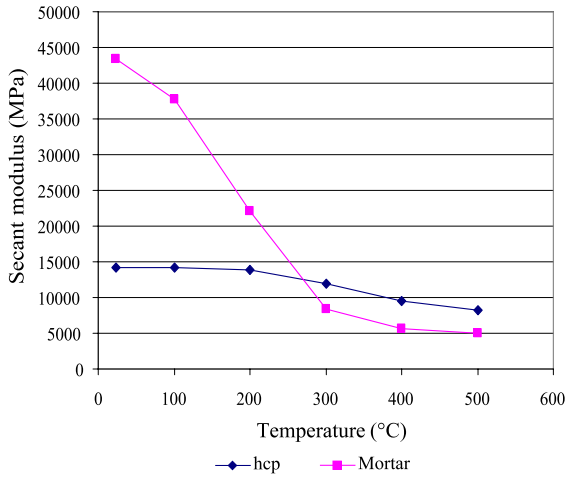

(b) Secant modulus vs. temperature

Fig. 9. Compressive peak strength and secant modulus of HCP and mortar at elevated temperatures up to 500 °C.

temperatures. As compared with the respective peak strengths at the room temperature, the peak strength loss of the HCP specimens was about 27% at 500 °C, and that of the mortar specimens was about 66%. Similarly, the reductions of the secant modulus of the HCP and the mortar specimens were about 43% and 89% respectively. The deterioration of the mechanical properties of the HCP specimens basically was due to the thermal decomposition of hydrates and the occurrence of dehydration-induced cracks. The consistent poorer mechanical performance of the mortar specimens than the HCP specimens was attributed to the development and accumulation of macrocracks, derived from the thermal mismatch between the HCP and the sand aggregates.

Within the temperature range (from room temperature to 500 °C) studied in this research, the strains corresponding to the peak-strength of the HCP specimens were around 0.6% at 500 °C. However, for the mortar specimens, these strain values increased from 0.2% at the room temperature to 0.65% at 500 °C. This observation was consistent with the

degradation of the secant modulus of the specimens. Therefore, among the mentioned thermal damage echanisms, thermal mismatch between the HCP and sand aggregates played a major role in the stiffness softening of the mortar specimens at elevated temperatures. It should be noted that for mortar, a nonlinear ascending branch before peak strength was observed in the temperature-dependent stress–strain curves, whereas for HCP, the ascending branch before peak strength almost maintained linear. This is probably because of the further development of thermal cracks resulting from the thermal mismatch between the HCP and the sand aggregates.

5. Discussions

Apart from the non-stress-induced thermal decomposition of hydration products as reported in literature [15–17], the dehydration-induced cracks, which were probably caused by the thermal mismatch of expansion/shrinkage among the different hydration products, was believed to be another factor affecting the mechanical properties of HCP under high temperatures. These microcracks were formed below 100 °C and grew rapidly with increasing temperatures. Above 200 °C, an intense crack pattern was developed (see Fig. 4). This also implies that the variation of the pore size and porosity of the HCP [1,13] is not sufficient to qualify/quantify the thermal damage of the HCP.

A mortar was prepared by mixing cement with fine aggregates. When a mortar specimen was subjected to high temperatures, macrothermal cracks appeared as a result of the increasing mismatch of expansion/shrinkage between the HCP and the aggregates, the strength-weakening decomposition of hydrates, and dehydration-induced cracks. The rapid growth of the macrocrack intensity made the mortars more vulnerable to strength loss than the companion HCP.

Because of the unique thermal characteristics of a HCP expansion at lower temperatures and contraction at higher temperatures, three types of cracks were formed in the HCP matrix or the aggregate inclusions at different temperatures (see Fig. 5). It had been shown that the sand aggregates generally had a lower linear coefficient of thermal expansion than the HCP at a temperature below 100 °C. Consequently, radial tensile stresses led to the formation of tangential cracks around the sand inclusions if the HCP–sand interface bond was weak, or inclusion cracks was formed if the inclusion strength was low. Further increase in temperatures made the HCP shrink. Consequently, the radial tensile stressed regions changed to be compressive and the tangential stresses were in tension, so that the bursting stresses around the sand inclusions eventually caused the development of radial cracks. The formation of tangential cracks, inclusion cracks and radial cracks due to thermal mismatch lead to a dramatic degradation of the mechanical properties of the mortar/concrete in a macroscale.

From the compressive stress–strain curves obtained in this study, the degradations of peak strength and secant modulus of the HCP were much less than those of the companion mortar specimens. Thus, the mismatch of expansion/shrinkage between the phase materials (HCP and aggregates) contributes more thermal damages in a composite material (i.e., mortar or concrete) than that experienced by an individual phase materials (i.e., HCP). It is also expected that the relative proportions of the phase materials in the composite affect the extent of and the contribution of each phase material in the overall thermal damage.

To perform a reliable numerical simulation of the thermal damage of a cement-based composite material, it is necessary to have realistic estimations of the temperature-dependent mechanical and more importantly expansion/shrinkage properties of each phase material (HPC, aggregates) in the formulation of the material models. This paper outlined a feasible method to determine the temperature-dependent mechanical properties of HCP solely due to the decomposition of hydrates and dehydration-induced cracks. The authors have incorporated the current findings to formulate a thermo-elastic damage model [10] for the numerical simulation of a cement-based composite under high temperatures. The simulation is being verified using the experimentally obtained stress–strain relations of the heated companion mortar specimens, and details of which will be reported in another paper.

6. Conclusions

In the present study, the changes in microstructure and mechanical properties of a predried hardened cement paste (HCP) and mortar specimens were successfully observed/measured, in a real-time mode, under elevated temperatures up to 500 °C. The main findings are summarized as follows:

1. The SEM examinations revealed that the thermal damage of HCP was not solely due to the thermal decomposition of hydrates but also to the development of the dehydration-induced cracks, which were probably caused by the thermal mismatch of the different constituent compounds of the HCP.
2. The thermal damage of the mortar was caused by the dehydration, the dehydration-induced cracks and the thermal cracks (tangential, radial, and inclusion) derived from the thermal mismatch between the HCP and the aggregate inclusions. Hence, mortar had a higher reduction rate of mechanical properties than HCP at elevated temperatures.
3. Regarding the temperature-dependent stress–strain relations, the ascending branch of HCP maintained relatively linear up to the peak-strength level. However, the ascending branch of mortar became nonlinear as the peak-strength level was approached. The nonlinearity was probably due to further propagation of thermal

cracks derived from the thermal mismatch between the HCP and the sand aggregates.

Acknowledgements

The materials presented in this paper are some of the findings of the G-V848 research project entitled ‘‘Thermal Stress and Associated Damage in Concrete at Elevated Temperatures’’ of The Hong Kong Polytechnic University. The authors would also like to thank Dr.Wang Xi-shu of Tsing Hua University for his technical support on the operation of the HTFTM test equipment.

References

[1] G.A. Khoury, Compressive strength of concrete at high temperatures: a reassessment, Mag. Concr. Res. 44 (161) (1992) 291–309.
[2] Comite Euro-international Du Beton, Fire design of concrete structures, in accordance with CEB/FIP model code 90 (final draft), Bulletin D’Information 208 (1991) (Switzerland).
[3] L.T. Phan, N.J. Carino, A review of mechanical properties of HSC at elevated temperature, J. Mater. Civ. Eng. 10 (1) (1998) 58–64.
[4] J. Piasta, Heat deformations of cement phases and microstructures of cement paste. Materials and structures: research and testing, RILEM 17 (102) (1984) 415–420.
[5] W.P.S. Dias, Time dependent deformations of hardened cement paste from 20 °C to 725 °C, PhD thesis, University of London, 1986.
[6] W.M. Lin, T.D. Lin, L.J. Powers-Couche, Microstructures of fire-damaged concrete, ACI Mater. J. 93 (3) (1996) 199–205.
[7] S.K. Handoo, S. Agarwal, S.K. Agarwal, Physicochemical, mineralogical, and morphological characteristics of concrete exposed to elevated temperatures, Cem. Concr. Res. 32 (7) (2002) 1009–1018.
[8] G.A. Khoury, P.J.E. Sullivan, B.N. Grainger, Radial temperature distributions within solid concrete cylinders under transient thermal states, Mag. Concr. Res. 36 (128) (1984) 146–156.
[9] F.H. Wittmann, Creep and shrinkage mechanisms, in: Z.P. Bazant, F.H. Wittmann (Eds.), Creep and Shrinkage in Concrete Structures, 1982, pp. 129–161, New York.
[10] Y.F. Fu, Y.L. Wong, C.A. Tang, C.S. Poon, Thermal induced stress and associated cracking in cement-based composite at elevated temperatures—Part I: Thermal cracking around single inclusion, Cem. Concr. Compos. (2003) (in press).
[11] Y.F. Fu, Y.L. Wong, C.A. Tang, C.S. Poon, Thermal induced stress and associated cracking in cement-based composite at elevated temperatures—Part II: Thermal cracking around multiple inclusions, Cem. Concr. Compos. (2003) (in press).
[12] X.J. Li, Z.J. Li, M. Onofrei, G. Ballivy, K.H. Khayat, Microstructural characteristics of HPC under different thermo-mechanical and thermo-hydraulic conditions, Mat. Struct. 32 (224) (1999) 727–733.
[13] F. Simonin, H. Elaqra, C. Olagnon, G. Fantozzi, Thermal conductivity and mechanical properties related to microstructure of a high alumina refractory castable, Silic. Ind. 66 (3–4) (2001) 33–39.
[14] G.J. Verbeck, W.E. Hass, Portland Cement Association, dilatometer method for determination of thermal coefficient of expansion of fine and coarse aggregate, in: R.W. Crun, F. Burggraf, J.R. Carey (Eds.), Proceedings of The 13th Annual Meeting, Highway Research Board, Division of Engineering and Industrial Research, National Research Council, Washington, DC, 1951, pp. 187–193.
[15] W.T. Chang, C.T. Wang, C.W. Huang, Concrete at temperatures above 1000 °C, Fire Saf. J. 23 (1994) 223–243.
[16] G.F. Peng, Evaluation of fire damage to high performance concrete, PhD thesis, The Hong Kong Polytechnic University, Hong Kong, 1999.
[17] Z.P. Bažant, M.F. Kaplan, Concrete at High Temperatures: Material Properties and Mathematical Models, Longman Group, England, 1996.